

# Interleukin-17 Impairs Salivary Tight Junction Integrity in Sjögren's Syndrome

L.W. Zhang<sup>1\*</sup>, X. Cong<sup>2\*</sup>, Y. Zhang<sup>2</sup>, T. Wei<sup>3</sup>, Y.C. Su<sup>2</sup>, A.C.A. Serrão<sup>2,4</sup>,  
A.R.T. Brito Jr.<sup>2,4</sup>, G.Y. Yu<sup>3</sup>, H. Hua<sup>1</sup>, and L.L. Wu<sup>2</sup>

## Abstract

Sjögren's syndrome (SS) is an inflammatory autoimmune disease that causes secretory dysfunction of the salivary glands. It has been reported that proinflammatory cytokine interleukin-17 (IL-17) was elevated and tight junction (TJ) integrity disrupted in minor salivary glands from SS patients. However, whether the elevated IL-17 in SS affects TJ integrity and thereby alters the function of salivary gland is unknown. Here, by using nonobese diabetic (NOD) mice as SS model, we found that the stimulated salivary flow rate was significantly decreased in NOD mice. Lymphocyte infiltration was mainly observed in submandibular glands (SMGs), but not parotid glands (PGs), of NOD mice. IL-17 was significantly increased and mainly located in lymphocytic-infiltrating regions in SMGs but not detectable in PGs of NOD mice. Meanwhile, the epithelial barrier function was disrupted, as evidenced by an increased paracellular tracer clearance and an enlarged acinar TJ width in SMGs of NOD mice. Furthermore, claudin-1 and -3 were elevated especially at the basolateral membranes, whereas claudin-4, occludin, and zonula occludens-1 (ZO-1) were reduced in SMGs of NOD mice. Moreover, occludin and ZO-1 were dispersed into cytoplasm in SMGs of NOD mice. However, no change in the expression and distribution of TJ proteins was found in PGs. In vitro, IL-17 significantly decreased the levels and apical staining of claudin-4 and ZO-1 proteins in the cultured SMG tissues, as well as claudin-1, occludin, and ZO-1 in PG tissues. Moreover, IL-17 activated the phosphorylation of I $\kappa$ B $\alpha$  and p65 in SMG cells, whereas pretreatment with NF- $\kappa$ B inhibitor pyrrolidine dithiocarbamate suppressed the IL-17-induced downregulation of claudin-4 and ZO-1 in SMG tissues. Taken together, these findings indicate that IL-17 derived from infiltrating lymphocyte impairs the integrity of TJ barrier through NF- $\kappa$ B signaling pathway, and thus might contribute to salivary gland dysfunction in SS.

**Keywords:** nonobese diabetic mice, submandibular gland, parotid gland, claudins, occludin, zonula occludens-1

## Introduction

Sjögren's syndrome (SS) is a chronic autoimmune disease characterized by periductal and perivascular infiltration of lymphocytes in exocrine glands, especially in salivary and lacrimal glands. The ensuing hyposalivation and hypolacrimation could lead to xerostomia and xerophthalmia, which severely affect systemic health and quality of life (Luciano et al. 2015). Despite ongoing efforts to explore the autoimmune basis of SS, the underlying etiology remains elusive. Previous studies suggest that genetic factors, environmental events, innate and adaptive immunities, and hormonal mechanisms are elements relevant to the pathogenesis of SS (Nikolov and Illei 2009).

Interleukin-17 (IL-17) is a proinflammatory cytokine associated with pathology in numerous autoimmune and inflammatory conditions, such as rheumatoid arthritis, multiple sclerosis, Crohn's disease, and systemic lupus erythematosus (Tesmer et al. 2008). Recently, a growing number of reports have considered IL-17 a potential pathogenic factor for SS. The expression of IL-17 in plasma and labial salivary glands from SS patients is elevated. Moreover, IL-17 is mainly expressed in the circumference of lymphoid infiltration focus, and its level elevates as the degree of lymphocyte infiltration increases (Katsifis et al. 2009; Mieliauskaitė et al. 2012; Fei et al. 2014).

Tight junctions (TJs) are multifunctional protein complexes localized in the apical region of the lateral membrane, including transmembrane proteins, such as claudin family members and occludin, as well as cytosolic proteins, such as zonula

<sup>1</sup>Department of Oral Medicine and Center for Salivary Gland Diseases of Peking University School and Hospital of Stomatology, Beijing, P.R. China

<sup>2</sup>Department of Physiology and Pathophysiology, Peking University Health Science Center, Key Laboratory of Molecular Cardiovascular Sciences, Ministry of Education, and Beijing Key Laboratory of Cardiovascular Receptors Research, Beijing, P.R. China

<sup>3</sup>Department of Oral and Maxillofacial Surgery, Peking University School and Hospital of Stomatology, Beijing, P.R. China

<sup>4</sup>Department of Dentistry, Santa Cecília University, Santos, Brazil

\*Authors contributing equally to this article.

A supplemental appendix to this article is published electronically only at <http://jdr.sagepub.com/supplemental>.

## Corresponding Authors:

H. Hua, Department of Oral Medicine, Peking University School and Hospital of Stomatology, Beijing, 100081, P.R. China.

Email: honghua1968@aliyun.com

L. L. Wu, Department of Physiology and Pathophysiology, Peking University Health Science Center, Beijing, 100191, P.R. China.

Email: pathophy@bjmu.edu.cn

occludens-1 (ZO-1; Zhang et al. 2013). By constituting a well-regulated diffusion barrier, TJs are crucial for the exchange of water, solute, and material through the paracellular pathway. Therefore, TJs are mostly considered important biomarkers of epithelial barrier function (Baker 2010). Previous studies indicate that disruption in TJ integrity is seen in minor salivary glands from SS patients (Ewert et al. 2010). However, whether the elevated IL-17 in SS affects TJ integrity and thereby alters the function of salivary gland is unknown. The present study was designed to explore the effects of IL-17 on TJ properties in the submandibular gland (SMG) and parotid gland (PG) by using the nonobese diabetic (NOD) mouse model for SS.

## Materials and Methods

### Measurement of Saliva Secretion and Paracellular Tracer Flux Assay

Twelve-week-old female NOD and BALB/c mice were fasted for a minimum of 5 h with water ad libitum. Blood glucose measurements were routinely performed, and only NOD mice with blood glucose  $\leq 240$  mg/dL were included in this study. Whole saliva was collected for 10 min from the oral cavity, starting at 5 min after pilocarpine (0.5  $\mu\text{g/g}$ ) intraperitoneal injection under isoflurane anesthesia. For paracellular tracer flux assay, 4-kDa fluorescein isothiocyanate (FITC)-dextran (1.5 mg/g; Sigma-Aldrich, St. Louis, MO, USA) was injected into the right jugular vein 20 min before pilocarpine injection and followed by saliva collection. The amount of FITC-dextran transported into saliva (shown as FITC-dextran clearance) was measured as described previously (Kawedia et al. 2007). Then, SMGs and PGs were collected for the following analysis. All experimental procedures were approved by the Ethics Committee of Animal Research, Peking University Health Science Center, and complied with the "Guide for the Care and Use of Laboratory Animals" (publication No. 85-23, revised 1996; National Institutes of Health, Bethesda, MD, USA). All animal research is reported in accordance with the ARRIVE (Animal Research: Reporting of In Vivo Experiments) guidelines (Kilkenny et al. 2010).

### Histopathologic, Immunohistochemical, and Immunofluorescence Staining

SMG and PG tissue sections (5  $\mu\text{m}$ ) were fixed in 4% paraformaldehyde; stained with hematoxylin and eosin or primary antibodies to IL-17, claudin-1, -3, -4 (Bioworld Technology, Saint Louis Park, MN, USA), and IL-17F (Proteintech, Chicago, IL, USA) at 4 °C overnight; and then incubated with horseradish peroxidase (HRP)-conjugated secondary antibody (Zhongshan Laboratories, Beijing, China) at 37 °C for 2 h. Image analysis was performed with ImageJ software (National Institutes of Health) and the Leica 550IW system (Leica, Wetzlar, Germany) with 5 randomly chosen fields from each section. For immunofluorescence, specimens were incubated with antibodies to claudin-1, -3, occludin, and ZO-1 (Invitrogen,

Carlsbad, CA, USA) at 4 °C overnight and then incubated with FITC-conjugated secondary antibody or Alexa Fluor 594-conjugated claudin-4 (Invitrogen) at 37 °C for 2 h. Nuclei were stained with DAPI (4,6-diamidino-2-phenylindole). Fluorescence images were captured under confocal microscope (TCS SP8; Leica).

### Flow Cytometry

The single-cell suspensions of SMGs were prepared with Liberase TL (Roche Diagnostics, Mannheim, Germany) and stimulated with phorbol-12-myristate-13-acetate (50 ng/mL), ionomycin (1  $\mu\text{g/mL}$ ), and brefeldin A (10  $\mu\text{g/mL}$ ; Sigma-Aldrich) for 5 h. Surface was stained with CD4/APC-CY7, then fixed and permeabilized, followed by intracellular staining with IFN- $\gamma$ /PerCP-CY5.5 and IL-17/PE (all from eBioscience, San Diego, CA, USA). Cells were analyzed on a FACS Aria II Flow Cytometer (BD Biosciences, San Jose, CA, USA).

### Transmission Electron Microscopy

SMG and PG samples were fixed in 2% paraformaldehyde-1.25% glutaraldehyde. Ultrathin sections were stained with uranyl acetate and lead citrate, then examined with a transmission electron microscope (H-7000; Hitachi, Tokyo, Japan). The distance between neighboring TJs (shown as TJ width) from 5 sections of 10 randomly selected fields were measured and averaged by 2 blinded examiners using ImageJ software.

### Tissue and Cell Culture

SMGs and PGs isolated from BALB/c mice and SMG-C6 cells were cultured as previously described (Quissell et al. 1997; Su et al. 2014). Tissues or cells were treated with IL-17 (50 ng/mL; R&D Systems, Minneapolis, MN, USA) or pyrrolidine dithiocarbamate (100  $\mu\text{mol/L}$ ; BioVision, Milpitas, CA, USA) for the indicated times at 37 °C and then harvested for the following detection.

### Real-time Polymerase Chain Reaction

Total RNA was isolated, and cDNA was synthesized with the RevertAid First Strand cDNA Synthesis Kit (Thermo Fisher Scientific, Waltham, MA, USA). The primers used in this study are shown in the Appendix Table. Real-time polymerase chain reaction (PCR) was performed with the DyNAmo Color Flash SYBR Green qPCR Kit under Thermo PikoReal PCR Systems (Thermo Fisher Scientific).

### Western Blot Analysis

Total protein was extracted, and the concentration was measured by the Bradford method. Equal amounts of protein were separated on 10% sodium dodecyl sulfate polyacrylamide gel electrophoresis (SDS-PAGE); transferred to polyvinylidene

difluoride membranes; blocked with 5% nonfat milk; probed with antibodies to IL-17 receptor (IL-17R; Abcam, Cambridge, UK), IL-17A, claudin-1, -3, -4, occludin, ZO-1, and actin (Santa Cruz Biotechnology, Santa Cruz, CA, USA) at 4 °C overnight; and then incubated with HRP-conjugated secondary antibodies (Zhongshan Laboratories) at room temperature. Target proteins were detected by enhanced chemiluminescence reagent (Thermo Fisher Scientific Pierce, Rockford, IL, USA).

### Lactate Dehydrogenase Cytotoxicity Assay

The cell viabilities were determined by the LDH Cytotoxicity Assay Kit (Beyotime Institute of Biotechnology, Jiangsu, China) according to the manufacturer's instruction.

### Statistical Analysis

Data are shown as mean  $\pm$  SEM. Statistical analysis was performed by unpaired Student's *t* test between NOD and BALB/c groups or by 1-way analysis of variance followed by Bonferroni's test among multiple groups. Correlation was analyzed by Pearson's coefficient correlation analysis.  $P < 0.05$  was considered statistically significant.

## Results

### Evaluation of SS-like Characters in NOD Mice

Stimulated salivary flow rate was significantly decreased in NOD mice compared with age-matched BALB/c mice ( $P < 0.05$ ; Fig. 1A). Typical perivascular and periductal inflammatory cell foci were observed in SMGs, but not PGs, of all NOD mice (Fig. 1B).

### Alteration of IL-17 and IL-17R in NOD Mice

To explore the role of IL-17 in the development of SS, we measured the expression of IL-17 and its receptor. IL-17A and IL-17F are main subtypes of IL-17 family secreted by T helper 17 (Th17) lymphocytes. The level of IL-17A mRNA was significantly increased in SMGs but not detectable in PGs (Fig. 1C, D). The expressions of IL-17R mRNA and protein in SMGs and PGs were not altered between BALB/c and NOD mice (Fig. 1C–F). Immunohistochemical staining showed that IL-17A was mainly distributed in SMG ducts of BALB/c mice while hardly detectable in PGs. The expression of IL-17A was remarkably enhanced in the lymphocytes infiltrating regions of SMGs of NOD mice (Fig. 1G). Semiquantitative analysis and Western blot results further identified these results (Fig. 1H, I). The staining of IL-17F was also detected but weaker than that of IL-17A in SMG infiltrates of NOD mice (Appendix Fig. 1). Then we focused on the effect of IL-17A on SMG in the present work.

Furthermore, the digested SMG cells were stained for CD4, IFN- $\gamma$ , and IL-17, and the activities of Th subsets were determined by flow cytometry. The proportions of CD4<sup>+</sup> IFN- $\gamma$ <sup>+</sup> and CD4<sup>+</sup> IL-17<sup>+</sup> T cells were 2.74%  $\pm$  0.56% and 0.48%  $\pm$  0.09%

in BALB/c mice while significantly increased to 13.70%  $\pm$  1.84% and 2.57%  $\pm$  0.36% in NOD mice (Appendix Fig. 2).

### Alteration of TJ-based Barrier Function in NOD Mice

FITC-dextran clearance, an indicator of the paracellular barrier function, was significantly increased in NOD mice ( $P < 0.05$ ; Fig. 2A). In BALB/c mice, TJs were located in the most apical portion between neighboring cells and formed a slightly dilated distance under transmission electron microscope. The acinar TJ width of SMG in NOD mice was significantly enlarged compared with BALB/c mice (21.59  $\pm$  2.28 nm vs. 12.77  $\pm$  0.05 nm,  $P < 0.05$ ), whereas no difference was found in PGs between NOD and BALB/c mice (11.45  $\pm$  0.52 nm vs. 11.20  $\pm$  0.50 nm; Fig. 2B–E). By contrast, the ductal TJ distances did not differ in SMGs and PGs from BALB/c and NOD mice (Appendix Fig. 3). The results suggested that the function and structure of the submandibular epithelial barrier were impaired in NOD mice.

Claudin-1, -3, -4, occludin, and ZO-1 are 5 major TJ components that have been detected in human, rat, and mouse SMGs and PGs. Compared with BALB/c mice, only claudin-4 mRNA expression was significantly reduced in SMGs of NOD mice ( $P < 0.05$ ), whereas other transmembrane TJs, including claudin-1, -3, and occludin, as well as cytosolic ZO-1, were unaltered (Fig. 2F). In contrast, the mRNA levels of these TJ components were not changed in PGs (Fig. 2G). The levels of claudin-1 and -3 proteins were elevated, whereas the expressions of claudin-4, occludin, and ZO-1 were reduced (Fig. 2H–M). The expressions of these TJs were not altered in PGs (Fig. 2N–R).

Claudin-1, -3, occludin, and ZO-1 were mainly located at apicolateral membranes of acini and ducts, with some weaker staining of claudin-1 and -3 at the basolateral sides, while claudin-4 was mainly distributed in ducts of SMGs and PGs in BALB/c mice. In the areas proximal and distal to lymphocytic infiltration, the stainings of claudin-1 and -3 were still observed at the apical and basolateral membranes, but their intensities were significantly increased at the basolateral membranes in SMGs of NOD mice. The staining of claudin-4 was reduced in ducts, whereas occludin and ZO-1 staining at the apical membranes became dispersed into the cytoplasm of acini in SMGs of NOD mice (Fig. 3A). By contrast, no change in TJ protein distribution was found in PGs (Appendix Fig. 4A). In accordance with the immunostaining results, quantitative analysis further identified the same changes in TJ distribution (Fig. 3B, Appendix Fig. 4B).

To evaluate whether there is a causal effect between IL-17 levels and TJ disruption, we did correlation analysis between the expression of IL-17 and each TJ protein. The level of IL-17 was positively correlated with claudin-1 and -3, while negatively correlated with claudin-4, occludin, and ZO-1, in SMGs of NOD mice. The salivary flow rate was also correlated with the expression of claudin-1, -3, -4, and ZO-1 but not occludin (Appendix Fig. 5).

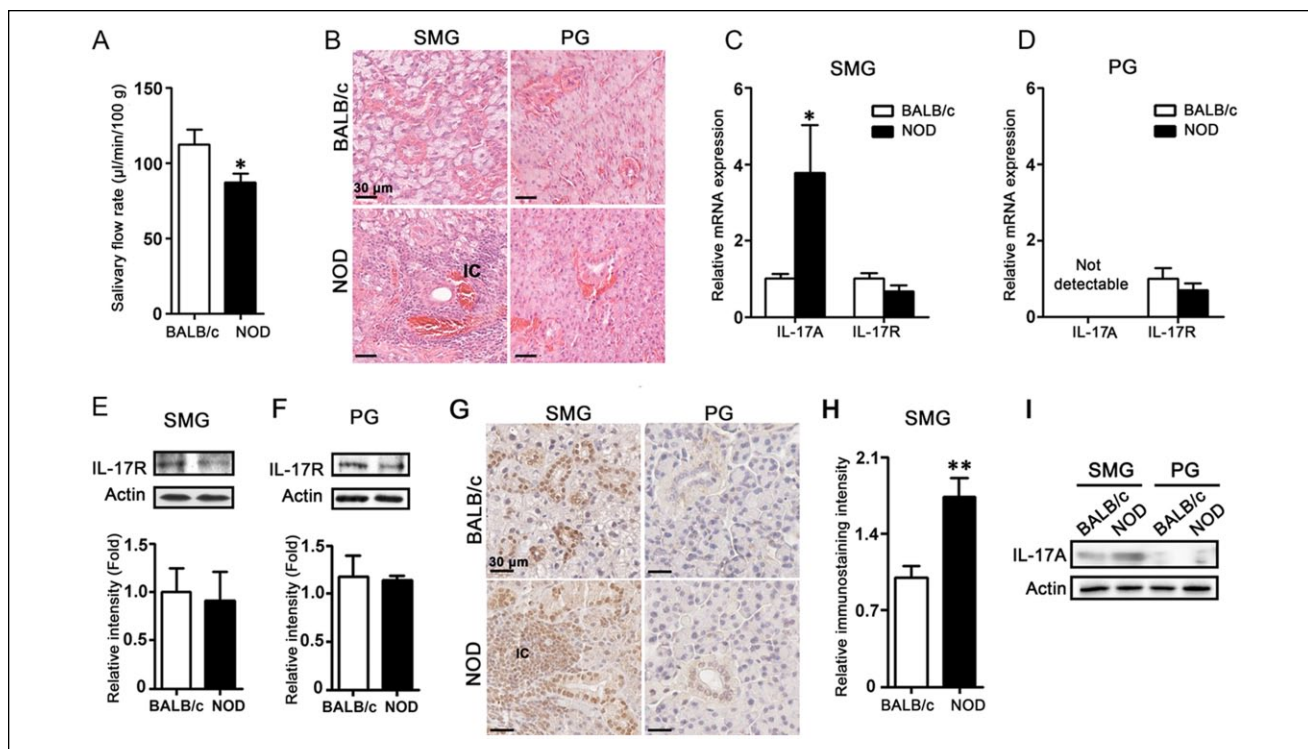


**Figure 1.** Evaluation of Sjögren's syndrome-like characters as well as the expression and distribution of interleukin-17 (IL-17) in nonobese diabetic (NOD) mice. The age-matched BALB/c mice were used as controls. **(A)** Whole saliva was collected for 10 min from the oral cavity starting at 5 min after pilocarpine (0.5 µg/g) intraperitoneal injection. The salivary flow rate was calculated as microliters per minute and per 100 g of body weight. **(B)** Histologic evaluation of submandibular gland (SMG) and parotid gland (PG) in BALB/c and NOD mice by hematoxylin and eosin staining. **(C, D)** The mRNA expression of IL-17A and IL-17R in SMGs and PGs. Quantification was normalized to GAPDH. **(E, F)** The expression of IL-17R in SMG and PG. Actin was used as a loading control. **(G)** Immunohistochemical staining of IL-17A in SMGs and PGs. **(H)** Quantification analysis of IL-17A in SMGs of BALB/c and NOD mice. **(I)** The expression of IL-17A in SMGs and PGs of BALB/c and NOD mice. All data are presented as mean  $\pm$  SEM of results from 6 mice in each group. \* $P < 0.05$  and \*\* $P < 0.01$  as calculated by the Student's *t* test. Scale bars: 30 µm. IC, infiltrating cells.

### Effect of IL-17 on TJs in SMG and PG Tissues

To explore whether the TJ changes in NOD mice was associated with IL-17, the fresh SMG and PG tissues from BALB/c mice were incubated with IL-17 (50 ng/mL). The levels of lactate dehydrogenase, an indicator of cellular damage, were not changed in culture medium of SMG or PG within 36 h (Appendix Fig. 6A, B). Besides, no difference was found in TJ mRNA levels in IL-17-untreated tissues among different time points (Appendix Fig. 6C–L). The mRNA expressions of claudin-4 and ZO-1, but not claudin-1, -3, or occludin, were decreased in SMG tissues after IL-17 treatment for 24 and 36 h, whereas only ZO-1 mRNA was downregulated in PGs (Fig. 4A–C, Appendix Fig. 7A–G). IL-17 also significantly decreased the protein levels of claudin-4 and ZO-1 in SMGs (Fig. 4D, E; Appendix Fig. 7H–K). The protein expressions of claudin-1, occludin, and ZO-1 were remarkably decreased by IL-17, whereas claudin-3 and -4 were unchanged in PGs (Fig. 4F–H, Appendix Fig. 7L–N).

In untreated SMG and PG tissues, TJ proteins were localized at the apicolateral or apicobasolateral membranes of acinar cells, except claudin-4 mainly expressed in ductal cells. IL-17 incubation for 36 h obviously decreased the apical intensities of claudin-4 and ZO-1 but did not affect claudin-1, -3, or

occludin in SMGs. Besides, IL-17 reduced claudin-1, occludin, and ZO-1 expression at apicolateral membranes, while claudin-3 and -4 were unaffected in PGs (Fig. 4I).

### Effect of IL-17 on NF- $\kappa$ B Signaling in Salivary Cells

We further explored the possible signaling molecule through which IL-17 modulated salivary epithelial TJs. After incubation with IL-17 (50 ng/mL), the levels of phosphorylated I $\kappa$ B $\alpha$  (p-I $\kappa$ B $\alpha$ ) were significantly increased, whereas the total levels of I $\kappa$ B $\alpha$  decreased in a rat SMG-C6 cell line. Meanwhile, there was a dramatic increase in the levels of p-p65 but no change in total p65 (Fig. 5A–E). Furthermore, pretreatment with pyrrolidone dithiocarbamate (100 µmol/L), a NF- $\kappa$ B inhibitor, suppressed the IL-17-induced downregulation of claudin-4 and ZO-1 in cultured SMGs (Fig. 5F–H).

### Discussion

In the present study, we identified that IL-17 derived from infiltrating lymphocyte was significantly increased, accompanied by structural and functional changes of TJ in SMGs of NOD

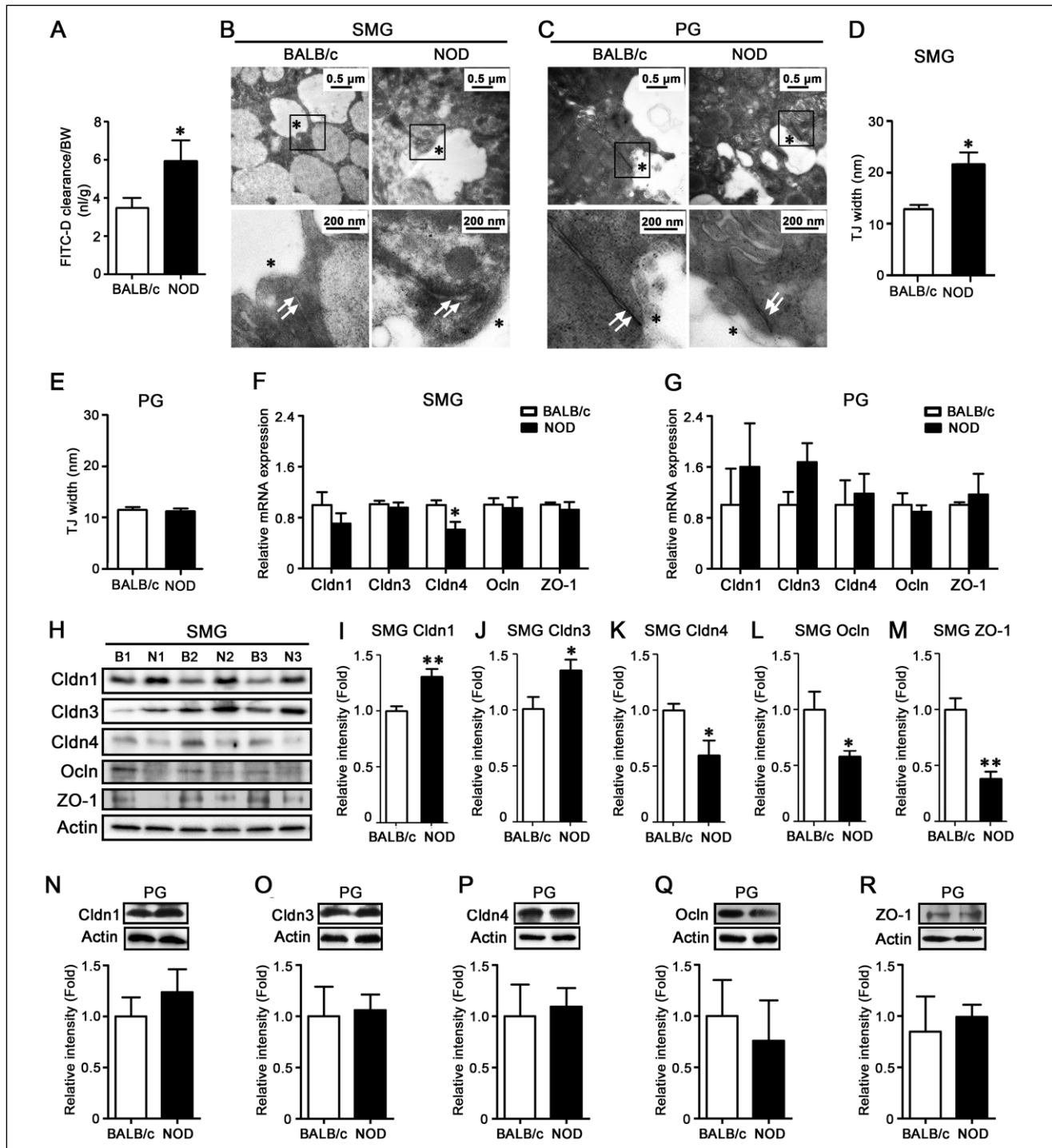


**Figure 2.** Assessment of the function, ultrastructure, and expression of tight junction (TJ) in nonobese diabetic (NOD) mice. **(A)** Measurement of paracellular permeability in salivary glands with 4-kDa FITC-dextran. FITC-dextran clearance was calculated as nanoliter and per gram of body weight. **(B, C)** Ultrastructure images of acinar TJs in submandibular glands (SMGs) and parotid glands (PGs) of BALB/c and NOD mice were observed under transmitted electron microscope. Boxed areas are shown at higher magnification in the lower panels. Arrows show TJs between neighboring acini. Scale bars: 0.5  $\mu$ m and 200 nm. **(D, E)** Quantitative analysis of the distance of neighboring acinar TJs (shown as TJ width) in SMGs and PGs of BALB/c and NOD mice. TJ width was calculated from 5 sections of 10 randomly selected fields. **(F, G)** The mRNA expression of claudin-1 (Cldn1), -3 (Cldn3), -4 (Cldn4), occludin (Ocln), and zonula occludens-1 (ZO-1) in SMGs and PGs. Quantification was normalized to GAPDH. **(H–R)** The expression of TJ proteins in SMG (H–M) and PG (N–R). Actin was used as a loading control. All data are presented as mean  $\pm$  SEM of results from 6 mice in each group. \* $P < 0.05$  and \*\* $P < 0.01$  as calculated by the Student's *t* test.

mice, whereas these alterations were not observed in PGs. Moreover, IL-17 could directly modulate TJ expression and distribution through the NF- $\kappa$ B signaling pathway in cultured salivary gland tissues and cells. These results demonstrate that IL-17 plays a critical role in impairing salivary TJ integrity and might be a potential therapeutic target in SS.

Recently, accumulating evidence indicates that pro-inflammatory cytokine IL-17 is involved in the pathogenesis of SS (Mieliuskaitė et al. 2012; Fei et al. 2014). A dominant population of IL-17-expressing cells is found within inflammatory lesions in minor salivary glands from SS patients as well as SMGs of SS mice. The local level of IL-17 is progressively increased with higher biopsy focus scores, which correlate with the severity of impairment in salivary gland structure and secretory function (Nguyen et al. 2008; Katsifis et al. 2009). IL-17 is significantly elevated in plasma from SS patients (Katsifis et al. 2009; Mieliuskaitė et al. 2012). Moreover, IL-17 adenovirus-mediated gene transfer induces histopathologic alterations of SS in BALB/c mice, and the therapeutic approach targeting IL-17 is effective to prevent salivary gland dysfunction (Nguyen et al. 2010; Nguyen et al. 2011; Lin et al. 2015). Here, we found that the local level of IL-17 was significantly increased in SMGs but not in PGs of NOD mice. Moreover, the elevated IL-17 was predominantly expressed within lymphocytic foci. Furthermore, the expression of IL-17R did not change in SMGs and PGs. Notably, we showed that CD4<sup>+</sup> IFN- $\gamma$ <sup>+</sup> Th1 cells accounted for a larger proportion than CD4<sup>+</sup> IL-17<sup>+</sup> Th17 cells in SMGs of NOD mice, implying that the role of Th1 lymphocytes should not be ignored. These results indicate that local inflammatory microenvironment plays an important role in the structure and function of salivary glands. Besides IFN- $\gamma$ , IL-17 derived from infiltrating lymphocyte is a critical inflammatory cytokine involved in salivary pathologic alteration of SS.

TJs function as a barrier to the diffusion of solutes through the paracellular pathway in various epithelia, and disruption in the TJ barrier is often seen in many inflammatory diseases, such as rheumatoid arthritis and inflammation bowel disease (Nishioku et al. 2011; Lameris et al. 2013). As a multiprotein complex, the imbalance in the expression and distribution of each TJ component contributes to TJ dysfunction. Overexpression of claudin-1 is associated with decreased paracellular permeability in MDCK cells, whereas claudin-1-deficient mice experience severe dehydration and die within 1 d after birth (Furuse et al. 2002). TNF- $\alpha$  selectively downregulated claudin-3 and increased paracellular permeability in SMG-C6 cells (Mei et al. 2015), suggesting a possible link between claudin-3 and paracellular transport in salivary glands. Claudin-4 is mainly expressed in ductal cells of salivary glands. Overexpression of

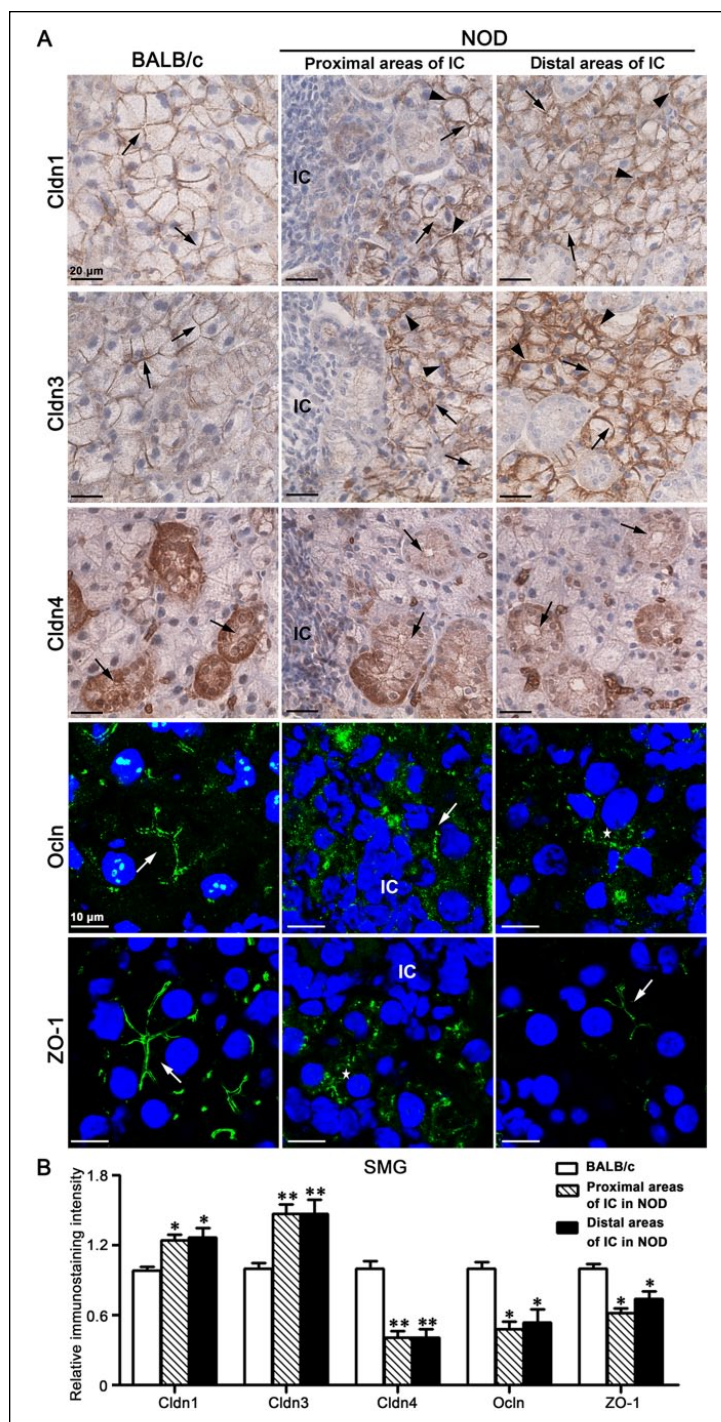


**Figure 3.** Distribution of tight junction proteins in submandibular gland (SMG) of BALB/c and nonobese diabetic (NOD) mice. **(A)** The immunostaining of claudin-1 (Cldn1), -3 (Cldn3), -4 (Cldn4), occludin (Ocln), and zonula occludens-1 (ZO-1) in SMGs. The areas proximal and distal to lymphocytic infiltration were both detected in SMGs of NOD mice. Cell nuclei were stained with either hematoxylin or DAPI (blue). Black or white arrows indicate the apicolateral membranes of acini or ducts. Black arrowheads indicate the basolateral membrane of acini, while white stars indicate the cytoplasm of acini. Scale bars: 20  $\mu$ m and 10  $\mu$ m. IC, infiltrating cells. **(B)** Quantitative analysis of tight junction staining intensities in BALB/c mice, with those in the areas proximal and distal to lymphocytic infiltration in SMGs of NOD mice. All data are presented as mean  $\pm$  SEM of results from 6 mice in each group. \* $P$  < 0.05 and \*\* $P$  < 0.01 compared with control. One-way analysis of variance was used among 3 groups.

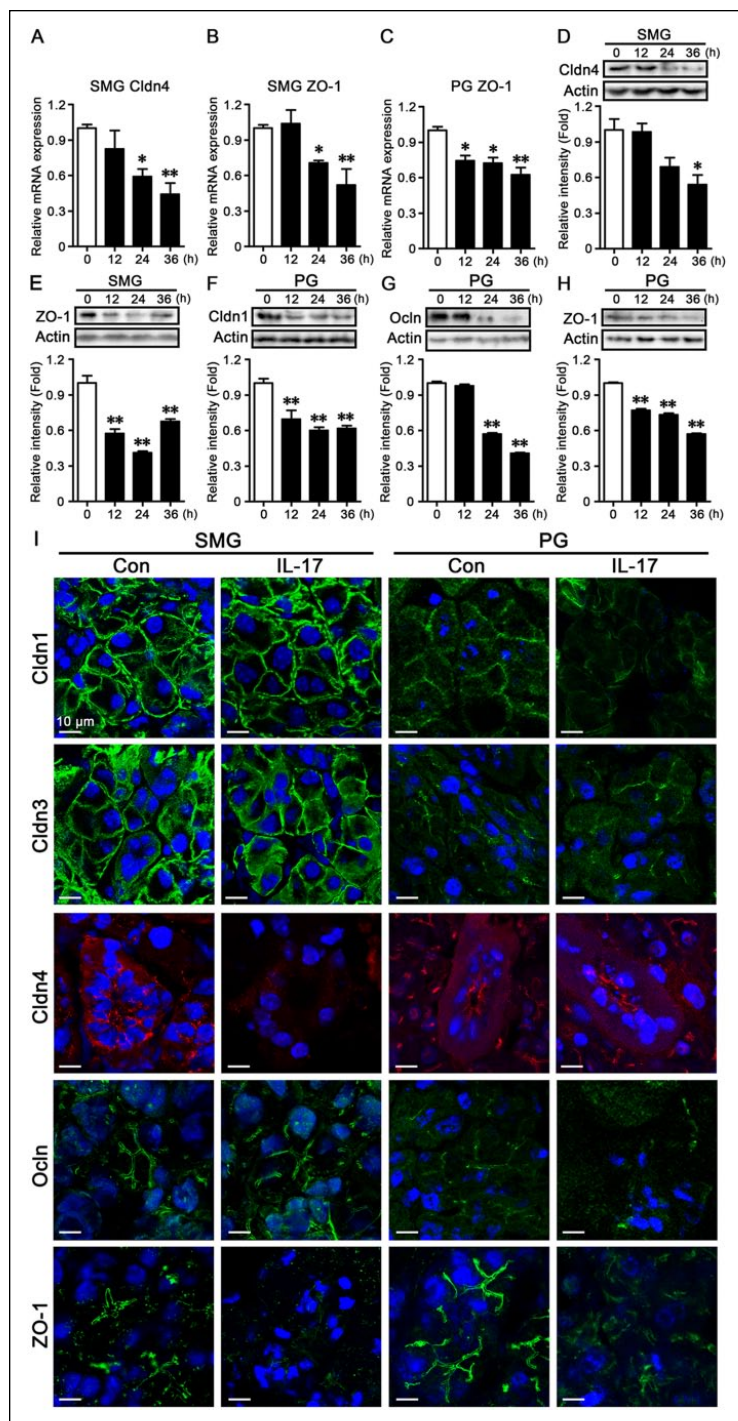


**Figure 4.** Effect of interleukin-17 (IL-17) on tight junction expression and distribution in cultured submandibular gland (SMG) and parotid gland (PG) tissues. SMGs and PGs from BALB/c mice were incubated with IL-17 (50 ng/mL) for the indicated times. **(A, B)** The mRNA expression of claudin-4 (Cldn4) and zonula occludens-1 (ZO-1) in SMG tissues. **(C)** The mRNA expression of ZO-1 in PG tissues. Quantification was normalized to GAPDH. **(D, E)** The expression and quantitative analysis of Cldn4 and ZO-1 proteins in SMG tissues. **(F–H)** The expression and quantitative analysis of claudin-1 (Cldn1), occludin (Ocln), and ZO-1 in PG tissues. Actin was used as a loading control. **(I)** Effect of IL-17 on tight junction distribution in cultured SMG and PG tissues. SMGs and PGs from BALB/c mice were treated with IL-17 (50 ng/mL) for 36 h. The immunofluorescence images of Cldn1, Cldn3, Cldn4, Ocln, and ZO-1 were taken under confocal microscope. Scale bars: 10  $\mu$ m. All experiments were performed for 4 independent experiments, and data are presented as mean  $\pm$  SEM. \* $P < 0.05$  and \*\* $P < 0.01$  compared with control. One-way analysis of variance was used among multigroups.

claudin-4 decreases paracellular permeability in rat submandibular SMIE cells, and claudin-4 is required for muscarinic acetylcholine receptor-induced paracellular permeability in SMG-C6 cells (Michikawa et al. 2008; Cong et al. 2015). Mice lacking occludin manifest loss of cytoplasmic granules in salivary striated ducts, while redistribution of occludin induced by capsaicin increases paracellular permeability (Saitou et al. 2000; Cong et al. 2013). ZO-1 is an indispensable cytoplasmic component that links the transmembrane TJs with actin cytoskeleton. In MDCK cells, the absence of ZO-1 results in a slight delay in TJ formation (McNeil et al. 2006). In salivary epithelium, ZO-1 and -2 play crucial roles in maintaining epithelial barrier function and transient receptor potential vanilloid subtype 1–modulated paracellular transport (Li et al. 2015). A recent study showed that local TNF- $\alpha$  produced in labial glands from SS patients altered TJ expression and distribution (Ewert et al. 2010). Here, we showed that the paracellular tracer clearance was increased and the acinar TJ width enlarged in SMGs of NOD mice, whereas these phenomena were not observed in PGs. The protein levels of claudin-4, occludin, and ZO-1 were significantly reduced, especially at the apicolateral membranes, whereas claudin-1 and -3 were obviously increased at the basolateral membranes of acinar cells. Since the alterations of TJ expression and distribution occur in only the lymphocytic-infiltrated and IL-17-elevated SMGs of NOD mice, these results suggest that the local inflammatory microenvironment, especially IL-17, might be responsible for TJ impairment.

Previous studies reported that IL-17 impairs the blood-brain and blood-testis barriers via downregulation of occludin and disrupts the intestinal barrier through upregulation of claudin-1 and -2 (Kinugasa et al. 2000; Huppert et al. 2010; Pérez et al. 2014). Here, by correlation analysis, we identified that there might be a causal effect between the expression of IL-17 and TJ proteins; moreover, the mice showing higher changes in TJs seemed to have the lower saliva production. To clarify the direct effects of IL-17 on TJ proteins of salivary glands, we cultured SMG and PG tissues with IL-17 in vitro. IL-17 significantly decreased the expression of claudin-4 and ZO-1, and their apical distributions were also impaired in SMGs. Because the same changes for claudin-4 and ZO-1 were seen in NOD mice, these results suggest that claudin-4 and ZO-1 might be the specific targets for IL-17 and play crucial roles in maintaining TJ integrity in SMGs. Notably, IL-17 could downregulate claudin-1, occludin, and ZO-1 in the cultured PG tissues, whereas TJ was unchanged in PGs of NOD mice, where no lymphocytic infiltration and IL-17 alteration were observed. These results further confirmed that IL-17 could directly modulate TJ expression and distribution in salivary

glands and that local IL-17 derived from infiltrating lymphocyte contributes to TJ barrier disruption in NOD mice.

Furthermore, we explored the signaling pathway that links IL-17 with TJs. NF- $\kappa$ B signaling is the classic downstream pathway activated by IL-17, and it can directly modulate TJ expression and distribution (Gaffen 2008; Berzal et al. 2015; Chen et al. 2015). Here, we found that IL-17 increased the levels of p-I $\kappa$ B $\alpha$  and p-p65 but decreased the levels of total I $\kappa$ B $\alpha$  in SMG-C6 cells. Pretreatment with NF- $\kappa$ B inhibitor abolished the IL-17-induced down-regulation of claudin-4 and ZO-1 in cultured SMGs, indicating that the effects of IL-17 on salivary TJs might be related with the activated NF- $\kappa$ B signaling pathway.

In summary, we demonstrate that the proinflammatory cytokine IL-17 derived from the infiltrated lymphocytes plays a crucial role in impairing the integrity of TJ barrier through NF- $\kappa$ B signaling pathway in NOD mice. These findings enriched our understanding of the pathogenic role of IL-17 in salivary epithelial cells and may provide new insights for the development of the therapeutic approaches for SS.

### Author Contributions

L.W. Zhang, X. Cong, contributed to data acquisition, analysis, and interpretation, drafted the manuscript; Y. Zhang, T. Wei, Y.C. Su, contributed to data analysis and interpretation, critically revised the manuscript; A.C.A. Serrão, A.R.T. Brito Jr, contributed to data acquisition, critically revised the manuscript; G.Y. Yu, H. Hua, L.L. Wu, contributed to conception and design, critically revised the manuscript. All authors gave final approval and agree to be accountable for all aspects of the work.

### Acknowledgments

We thank Dr. David O. Quissell from the School of Dentistry, University of Colorado Health Sciences Center, Denver, CO, USA, for the generous gift of rat SMG-C6 cell line, and Dr. Fan-Lei Hu from the Department of Rheumatology and Immunology, Peking University People's Hospital, Beijing, China, for the flow cytometry detection. This study was supported by the National Natural Science Foundation of China (grants 81371163 and 81300893). The authors declare no potential conflicts of interest with respect to the authorship and/or publication of this article.

### References

Baker OJ. 2010. Tight junctions in salivary epithelium. *J Biomed Biotechnol.* 2010:278948.

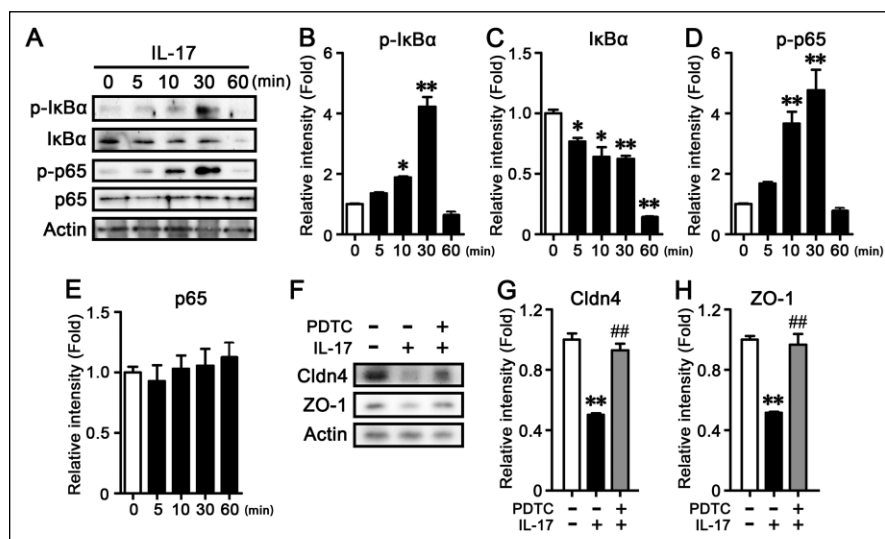


**Figure 5.** Effect of interleukin-17 (IL-17) on NF- $\kappa$ B signaling pathway. (A–E) The levels and quantitative analysis of phosphorylated I $\kappa$ B $\alpha$  (p-I $\kappa$ B $\alpha$ ), I $\kappa$ B $\alpha$ , phosphorylated p65 (p-p65), and p65 expressions induced by IL-17 (50 ng/mL) in rat SMG-C6 cell line. (F–H) Effect of IL-17 on the expression of claudin-4 (Cldn4) and zonula occludens-1 (ZO-1) by pretreatment with NF- $\kappa$ B inhibitor pyrrolidine dithiocarbamate (PDTC; 100  $\mu$ mol/L) in cultured submandibular gland tissues from BALB/c mice. All experiments were performed for 4 independent experiments, and data are presented as mean  $\pm$  SEM. \* $P$  < 0.05 and \*\* $P$  < 0.01 compared with control. ### $P$  < 0.01 compared with IL-17-treated cells. One-way analysis of variance was used among multigroups.

- Berzal S, González-Guerrero C, Rayego-Mateos S, Uccero Á, Ocaña-Salceda C, Egidio J, Ortiz A, Ruiz-Ortega M, Ramos AM. 2015. TNF-related weak inducer of apoptosis (TWEAK) regulates junctional proteins in tubular epithelial cells via canonical NF- $\kappa$ B pathway and ERK activation. *J Cell Physiol.* 230(7):1580–1593.
- Chen SW, Zhu J, Zuo S, Zhang JL, Chen ZY, Chen GW, Wang X, Pan YS, Liu YC, Wang PY. 2015. Protective effect of hydrogen sulfide on TNF- $\alpha$  and IFN- $\gamma$ -induced injury of intestinal epithelial barrier function in Caco-2 monolayers. *Inflamm Res.* 64(10):789–797.
- Cong X, Zhang Y, Li J, Mei M, Ding C, Xiang RL, Zhang LW, Wang Y, Wu LL, Yu GY. 2015. Claudin-4 is required for modulation of paracellular permeability by muscarinic acetylcholine receptor in epithelial cells. *J Cell Sci.* 128(12):2271–2286.
- Cong X, Zhang Y, Yang NY, Li J, Ding C, Ding QW, Su YC, Mei M, Guo XH, Wu LL, et al. 2013. Occludin is required for TRPV1-modulated paracellular permeability in the submandibular gland. *J Cell Sci.* 126(Pt 5):1109–1121.
- Ewert P, Aguilera S, Alliende C, Kwon YJ, Albornoz A, Molina C, Urzúa U, Quest AF, Olea N, Pérez P, et al. 2010. Disruption of tight junction structure in salivary glands from Sjögren's syndrome patients is linked to proinflammatory cytokine exposure. *Arthritis Rheum.* 62(5):1280–1289.
- Fei Y, Zhang W, Lin D, Wu C, Li M, Zhao Y, Zeng X, Zhang F. 2014. Clinical parameter and Th17 related to lymphocytes infiltrating degree of labial salivary gland in primary Sjögren's syndrome. *Clin Rheumatol.* 33(4):523–529.
- Furuse M, Hata M, Furuse K, Yoshida Y, Haratake A, Sugitani Y, Noda T, Kubo A, Tsukita S. 2002. Claudin-based tight junctions are crucial for the mammalian epidermal barrier: a lesson from claudin-1-deficient mice. *J Cell Biol.* 156(6):1099–1111.
- Gaffen SL. 2008. An overview of IL-17 function and signaling. *Cytokine.* 43(3):402–407.
- Huppert J, Closhen D, Croxford A, White R, Kulig P, Pietrowski E, Bechmann I, Becher B, Luhmann HJ, Waisman A, et al. 2010. Cellular mechanisms of IL-17-induced blood-brain barrier disruption. *FASEB J.* 24(4):1023–1034.
- Katsifis GE, Rekka S, Moutsopoulos NM, Pillemer S, Wahl SM. 2009. Systemic and local interleukin-17 and linked cytokines associated with Sjögren's syndrome immunopathogenesis. *Am J Pathol.* 175(3):1167–1177.
- Kawedia JD, Nieman ML, Boivin GP, Melvin JE, Kikuchi K, Hand AR, Lorenz JN, Menon AG. 2007. Interaction between transcellular and paracellular water transport pathways through Aquaporin 5 and the tight junction complex. *Proc Natl Acad Sci U S A.* 104(9):3621–3626.

- Kilkenny C, Browne WJ, Cuthill IC, Emerson M, Altman DG. 2010. Improving bioscience research reporting: the ARRIVE guidelines for reporting animal research. *J Pharmacol Pharmacother.* 1(2):94–99.
- Kinugasa T, Sakaguchi T, Gu X, Reinecker HC. 2000. Claudins regulate the intestinal barrier in health and during inflammatory bowel disease. *Gastroenterology.* 118(6):1001–1011.
- Lameris AL, Huybers S, Kaukinen K, Mäkelä TH, Bindels RJ, Hoenderop JG, Nevalainen PI. 2013. Expression profiling of claudins in the human gastrointestinal tract in health and during inflammatory bowel disease. *Scand J Gastroenterol.* 48(1):58–69.
- Li J, Cong X, Zhang Y, Xiang RL, Mei M, Yang NY, Su YC, Choi S, Park K, Zhang LW, et al. 2015. ZO-1 and -2 are required for TRPV1-modulated paracellular permeability. *J Dent Res.* 94(12):1748–1756.
- Lin X, Rui K, Deng J, Tian J, Wang X, Wang S, Ko KH, Jiao Z, Chan VS, Lau CS, et al. 2015. Th17 cells play a critical role in the development of experimental Sjögren's syndrome. *Ann Rheum Dis.* 74(6):1302–1310.
- Luciano N, Valentini V, Calabrò A, Elefante E, Vitale A, Baldini C, Bartoloni E. 2015. One year in review 2015: Sjögren's syndrome. *Clin Exp Rheumatol.* 33(2):259–271.
- McNeil E, Capaldo CT, Macara IG. 2006. Zonula occludens-1 function in the assembly of tight junctions in Madin-Darby canine kidney epithelial cells. *Mol Biol Cell.* 17(4):1922–1932.
- Mei M, Xiang RL, Cong X, Zhang Y, Li J, Yi X, Park K, Han JY, Wu LL, Yu GY. 2015. Claudin-3 is required for modulation of paracellular permeability by TNF- $\alpha$  through ERK1/2/slug signaling axis in submandibular gland. *Cell Signal.* 27(10):1915–1927.
- Michikawa H, Fujita-Yoshigaki J, Sugiya H. 2008. Enhancement of barrier function by overexpression of claudin-4 in tight junctions of submandibular gland cells. *Cell Tissue Res.* 334(2):255–264.
- Mieliauskaitė D, Dumalakiene I, Ruginė R, Mackiewicz Z. 2012. Expression of IL-17, IL-23 and their receptors in minor salivary glands of patients with primary Sjögren's syndrome. *Clin Dev Immunol.* 2012:187258.
- Nguyen CQ, Hu MH, Li Y, Stewart C, Peck AB. 2008. Salivary gland tissue expression of interleukin-23 and interleukin-17 in Sjögren's syndrome: findings in humans and mice. *Arthritis Rheum.* 58(3):734–743.
- Nguyen CQ, Yin H, Lee BH, Carcamo WC, Chiorini JA, Peck AB. 2010. Pathogenic effect of interleukin-17A in induction of Sjögren's syndrome-like disease using adenovirus-mediated gene transfer. *Arthritis Res Ther.* 12(6):R220.
- Nguyen CQ, Yin H, Lee BH, Chiorini JA, Peck AB. 2011. IL17: potential therapeutic target in Sjögren's syndrome using adenovirus-mediated gene transfer. *Lab Invest.* 91(1):54–62.
- Nikolov NP, Illei GG. 2009. Pathogenesis of Sjögren's syndrome. *Curr Opin Rheumatol.* 21(5):465–470.
- Nishioku T, Furusho K, Tomita A, Ohishi H, Dohgu S, Shuto H, Yamauchi A, Kataoka Y. 2011. Potential role for S100A4 in the disruption of the blood-brain barrier in collagen-induced arthritic mice, an animal model of rheumatoid arthritis. *Neuroscience.* 189:286–292.
- Pérez CV, Pellizzari EH, Cigorraga SB, Galardo MN, Naito M, Lustig L, Jacobo PV. 2014. IL17A impairs blood-testis barrier integrity and induces testicular inflammation. *Cell Tissue Res.* 358(3):885–898.
- Quissell DO, Barzen KA, Gruenert DC, Redman RS, Camden JM, Turner JT. 1997. Development and characterization of SV40 immortalized rat submandibular acinar cell lines. *In Vitro Cell Dev Biol Anim.* 33(3):164–173.
- Saitou M, Furuse M, Sasaki H, Schulzke JD, Fromm M, Takano H, Noda T, Tsukita S. 2000. Complex phenotype of mice lacking occludin, a component of tight junction strands. *Mol Biol Cell.* 11(12):4131–4142.
- Su YC, Xiang RL, Zhang Y, Ding C, Cong X, Guo XH, Yang NY, Hua H, Wu LL, Yu GY. 2014. Decreased submandibular adiponectin is involved in the progression of autoimmune sialoadenitis in non-obese diabetic mice. *Oral Dis.* 20(8):744–755.
- Tesmer LA, Lundy SK, Sarkar S, Fox DA. 2008. Th17 cells in human disease. *Immunol Rev.* 223:87–113.
- Zhang GH, Wu LL, Yu GY. 2013. Tight junctions and paracellular fluid and ion transport in salivary glands. *Chin J Dent Res.* 16(1):13–46.